ASTR 4017/8007: Diffuse Matter in the Universe

Class 1 Notes: Introduction; Collisional processes

The subject of this class is the low density gas between the stars and galaxies. Our goal will be to develop a physical understanding of how this material works. The physics that governs it is all familiar and has been understood for at least the last fifty years – gas dynamics, radiation, some quantum mechanics – but the low densities found in interstellar space provide a completely novel context far removed from any other physical regime we're used to thinking about. For this reason, many of the familiar behaviours we expect are absent or altered in the interstellar context. This makes the ISM a wonderfully complex and challenging problem.

The class is roughly divided into two parts. The first half covers the physics of the ISM, developing theories for the important processes that occur in low density gas. The second half applies those models to understand the behavior of the major constituents of the ISM and IGM. What we will cover does not even come close to being exhaustive. The ISM is still a young and rapidly-developing field of study. One omission in particular does deserve mention: we will spend almost no time discussing the ability of the ISM to form new stars, one of its most important properties. This is mainly because there is an entire other class devoted to that subject.

Although we will be starting with ISM physics and only later getting into applications, it is helpful to have in mind a rough phenomenology to guide us in picking characteristic numbers and scales, and in suggesting what problems are interesting. For this reason, the first part of today's class will be devoted to a brief phenomenology of the ISM and IGM. After that we will begin to set up the basic calculation machinery we will use for much of the remainder of the class.

Finally, a note on nomenclature: because saying "ISM and IGM" repeatedly would be tiresome, I am simply going to say "ISM" most of the time, with the understanding that this encompasses the IGM as well. I will try to be clear when I am saying something that applies only to the ISM or the IGM.

I. A brief history of the ISM

The very existence of the ISM was not realised until fairly late in the history of astronomy, and understanding of its nature is even more recent. This is in part because the ISM, except in rare circumstances, does not emit optical light. Those few objects that do emit in the optical were known as nebulae, and by 1860 the "New General Catalog" (as in NGC) based on the observations of William Herschel and his son John, contained more than 500 objects. Many of these were galaxies, but some were interstellar objects.

The first hints that at the nature of these interstellar objects came from observations made at Lick Observatory in California between 1860 and 1900 by W. Huggins and J. E. Keeler. ADS is actually pretty complete even this far back, so one can find the original papers quite easily. Keeler reported that spectra of nebulae showed that the light they emitted was entirely line emission, with no detectable underlying continuum. Moreover, the very narrow widths of the lines indicated low pressures, in contrast to stellar spectra.

[Slide 1 – Keeler PASP article]

A second hint came in 1904. When studying the spectrum of the binary star δ Orionis, J. Hartmann of Postdam noticed that, although all the other lines showed the expected periodic velocity shifts associated with orbital motion, the calcium II K line at 3934 Å did not vary at all. In addition, the line was extremely weak and extremely narrow. Hartmann considers and discards several explanations, before concluding that the line must be produced by a cloud between the stars and Earth.

[Slide 2 – Hartmann ApJ article]

Yet another piece of the puzzle arrived in 1919, when Barnard, also at Lick, published his catalog of dark clouds. The title of the paper is a wonderfully early 20th century one: "On the Dark Markings of the Sky, with a Catalogue of 182 Such Objects." Barnard noticed a series of dark regions where there were no stars.

[Slide 3 – Barnard ApJ article]

Of course the modern view is a bit more impressive...

[Slide 4 – B68 as seen today]

Arthur Eddington summarised much of the observations in 1926 in a lecture to the Royal Society in 1926 called "Diffuse Matter in Interstellar Space", in which he argued that the observed calcium lines in stars were of interstellar origin, and argued that the observed optical nebulae are simply the places where the ISM is dense and lit up by stars, and that they are part of a larger, more widespread medium. He also predicted the existence of H_2 molecules in space.

Incidentally, it's worth looking up the original papers from 1926, if only to read the wonderfully snippy exchange of letters by Jeans and Eddington published in *The Observatory* that followed the lecture. In essence Jeans was mad that Eddington had not cited his 1905 paper on what we now know as Jeans instability, while Jeans said that the paper was wrong as Jeans had originally tried to apply it, to determine the masses of stars. Astronomers complaining about not being cited is definitely not a new phenomenon...

Discoveries arrived quite quickly after that. In 1930, Robert Trumpler (also of Lick) showed that there was a systematic deviation between the luminosity and angular diameter distances of galactic clusters, with the luminosity distance coming out systematically larger for larger angular diameter distances. This could naturally be explained by the widespread presence of interstellar extinction of the stellar continuum, which would make distant cluster systematically dimmer. In the same year, Struve showed that Ca II K lines are stronger in more distant stars, again consistent with the idea of a widespread absorbing medium.

[Slide 5 – plot from Trumpler PASP article]

In the 1930s a series of additional absorption bands were discovered, some corresponding to diatomic molecules like CH, CH^+, and CN. Some were diffuse and weak, and they are still unidentified today – they likely arise from complex carbonaceous molecules, but the exact chemical composition is unknown.

The next big breakthrough was actually detecting the ISM directly, rather than via absorption of starlight, and this had to wait for the advent of radio astronomy. In 1944 Henk van de Hulst discovered the existence of the 21 cm hyperfine line of neutral hydrogen, and in 1951 Ewen and Purcell reported the first detection of interstellar H I. In the 1950s and 60s, a series of increasingly good maps of the galactic disk in 21 cm emission were made, leading to the realization that H I constitutes about 10% of the total mass of the galactic disk, adding up to about 5×10^9 $M_\odot$.

In 1966 Lynds & Stockton discovered the Lyman α forest produced by intergalactic H I absorption, and in 1968 the first polyatomic interstellar molecule, NH_3 (ammonia), was seen. This was followed by the detection of the 2.6 mm line of the CO molecule in 1970 by Wilson, Jefferts, & Penzias, leading to the discovery of another significant component of the ISM: molecular clouds, with a total mass also comparable to $\sim 10^9$ $M_\odot$.

Thereafter advances continued as instrumentation got faster. The launching of the first satellite detectors in the 1960s and 1970s led to discovery of soft background x-ray emission, produced by nearby gas at temperature of $\sim 10^6$ K. Subsequent x-ray missions such has Chandra and XMM led to the discovery of hot gas in distant galaxy clusters.

The Copernicus satellite launched in 1973 opened up the UV window, leading to the discovery of H_2 lines in absorption against stars, and emission lines from highly ionised atoms such as O IVin the hot gas. It also provided evidence for the depletion of refractory elements from the gas phase into solid grains. It was followed up by FUSE in 2000.

In 1983, the IRAS satellite did the same for infrared, providing an all-sky view at 12, 25, 60, and 100 μm, which mostly traces emission from small dust grains. In 1990 COBE, in addition to measuring the CMB, detected ubiquitous emission in the 158 μm line of C II. This turns out to be the most important cooling line for neutral gas. Later IR satellites including ISO, SWAS, Spitzer, and Herschel have provided even more information.

[Slide 6 – IRAS all-sky map]

The 1990s saw the development of ground-based interferometers, which were capable of imaging gas and dust emitting at mm wavelengths where the atmosphere is (from a good site) relatively transparent. One of the first of these were the Berkeley-Illinois-Maryland Array (BIMA), which provided some of the first maps of CO molecules outside the Milky Way. These culminated in the development of the Atacama Large Millimetre Array (ALMA) in the 2010s.

II. Components of the ISM – the present understanding

After that brief historical review, let's turn to the modern understanding of the ISM, which includes a lot more than just the gas we've talked about thus far. We can identify several components of the ISM in addition to gas.

A. Dust

One component to which we've already alluded is dust. A significant fraction of the refractory elements, i.e. those whose solid forms vaporize at temperature ~ 1000 K rather than ~ 100 K, are found not in the gas phase but as a small dust grains.

The fraction of such elements in grain rather than gas form varies with the ambient density and temperature, ranging from a majority of material being in grain form in dense and cold environments to almost none of it in hot environments. However even in extremely hot gas at temperatures of $\sim 10^6 - 10^7$ K some dust grains survive, mainly because the grains are not necessarily heated to anything close to the gas temperature – a point we will return to later in the course.

The size distribution of grain is somewhat uncertain, but it can be constrained by observations of the grains' absorption, scattering, and emission properties, since these are closely correlated with size. Roughly speaking the cross-section of a grain to light reaches a maximum for light whose wavelength is comparable to the grain size. For light of shorter wavelengths grain cross-sections are simply their physical sizes, while for light of longer wavelengths the cross-section declines roughly as the square of the ratio of grain size to wavelength. We will also return to this discussion later on. Based on these observations, the typical size of interstellar dust grains must be less than ~ 1 μm in size.

B. Cosmic rays

The gas in interstellar space mostly has a Maxwellian velocity distribution, as we will demonstrate in the next class. However, there are also ions and electrons that have much larger, typically relativistic velocities. These are referred to as cosmic rays. The most energetic ones detected have energies of $\sim 10^{21}$ eV, or $\sim 10^9$ erg. For comparison, the kinetic energy carried by a major league fastball (150 g ball traveling at 100 mph) is also about 10^9 erg.

The mechanism by which cosmic rays are accelerated to such speeds is still not completely understood, but it is thought to involve high-speed shocks produced by supernova, massive star winds, or similar phenomena. Regardless of the acceleration mechanism, though, once launched cosmic rays propagate long distances through the ISM. We will not discuss CRs much in this class, because they are covered extensively in the high-energy astrophysics class, except when they become important for understanding the way the ISM and IGM behave.

C. Photons

The ISM is also pervaded by photons of various frequencies. In addition to the ubiquitous CMB, there is mostly optical and UV light from stars, infrared radiation from dust grains, radio emission from hot gas, synchotron radiation from relativistic gas, and numerous line photons at frequencies ranging from radio to gamma rays produced by a huge number of molecules, atoms, ions, and nuclei.

D. Magnetic fields

As we shall see later on, much of the ISM is occupied by ionised gas, and even in regions where the gas is mostly neutral there is usually some weak residual ionisation produced by a number of processes we will discuss later. This means that the ISM can generally be thought of as an ideal plasma. Plasmas have the property that they can sustain magnetic fields, and any moving plasma invariably generates fields. The ISM is not exception.

Evidence for the magnetic field arises from numerous sources. First, starlight is polarised as well as extincted by interstellar dust grains. Producing a net polarisation is possible only if the grains have a large-scale alignment, and the only plausible candidate to produce this alignment is a large-scale magnetic field.

In addition, there are a number of atomic and molecular emission lines that are magnetically sensitive, meaning that the line shape, polarisation, or some other property of the line changes in the presence of a magnetic field. Such lines do generally indicate that a field is present.

III. ISM phases

Despite this menagerie of components, the ISM can be roughly organised into a number of characteristic phases, identified by a combination of temperature and the ionisation state of the hydrogen. For now we will simply assert this, and as we go through the course we will discuss the theoretical and observational justification for this division. An excellent quick-reference summary of the material is given in the first chapter of the textbook.

A. Hot gas (HIM)

The hottest component, and the dominant one outside the disks of galaxies and into the IGM, is hot gas, or HIM. This gas is also found within the galactic disk in places where the gas has been shocked by supernova blast waves, and it may occupy several tens of percent of the volume of the galactic disk.

Typical temperatures in this gas are 10^6 K or more. As these temperatures hydrogen is collisionally ionised, and numerous highly-ionised species of heavy elements are also present, for example O VI. The high temperatures ensure that the gas is able to expand easily until it reaches low densities, typically $\sim 10^{-3}$ cm^{-3} within the disk of the galaxy and even lower outside it.

At these temperatures the gas emits mostly in x-rays and UV, and by radio synchrotron emission from free electrons. X-ray emission also provides the main channel by which this gas is able to cool, although the cooling times can be extremely long due to the low densities. For much of the IGM, the cooling time is longer than the Hubble time.

B. Warm ionised gas (WIM) / H II

The next hottest phase, called the warm ionised medium or H II regions, is gas at temperatures of $\sim 10^4$ K – there is very little gas at intermediate temperatures of $\sim 10^5$ K because gas at that temperature tends to cool very rapidly.

At 10^4 K, $k_B T \sim 1$ eV, so the gas is not moving gas enough for the typical collision to induce ionisation (since the hydrogen ionisation potential is 13.6 eV). Instead, WIM gas is found near hot stars that provide high energy photons to photoionise the hydrogen. Regions in this state occupy $\sim 10\%$ of the volume of the galactic disk, and their typical densities are $1 - 100$ cm^{-3}, although there is a huge range of variation.

The photons that ionise the gas also provide the major source of energy to it. Each time an ionisation occurs by a photon that has an energy a bit above 13.6 eV, the resulting free electron acquires some excess kinetic energy, which it then thermalises by bouncing off the surrounding ions.

Countering this heating, gas at these temperatures cools by numerous processes. These include recombination radiation, which is produced when ionised hydrogen recombines into an excited state and then radiatively decays to the ground state, free-free emission from free electrons, and also a great deal of line emission produced by collisions between free electrons and partially ionised metal atoms. The line radiation produces spectacular optical emission, and for this reason H II regions are some of the most visually spectacular objects around. The famous Eagle Nebula HST images are of an H II region.

[Slide 7 – Eagle Nebula]

In addition to the visually spectacular H II regions, which represent the densest parts of the WIM, there are also numerous diffuse, low-density regions of ionised gas. These are not necessarily associated with young hot stars, and instead represent places where the gas was ionised once, and the density is low enough that only a little radiation is needed to keep it ionised, or where the recombination has not yet had time to occur.

C. Warm neutral gas (WNM)

In the absence of a local heat source like a hot star or a supernova blast, interstellar gas tends to become neutral, which brings us to our next phase: WNM, or warm neutral medium. The gas in this phase is generally at temperatures of $5,000 - 10,000$ K, and has a density not very different from that of the H II regions, $\sim 0.1 - 1$ cm^{-3}. Gas in this state occupies a large fraction of the volume of the galactic disk, $\sim 40\%$.

In this gas there are no photons above 13.6 eV to provide energy, but photons at somewhat lower energies provide a similar heating mechanism. Although such lower energy photons cannot ionise hydrogen, then can knock electrons off dust grains via the photoelectric effect, and this proves to be the dominant heating source.

Countering this heating, the WNM also contains numerous weakly ionised or neutral metal atoms that can be collisionally excited much like those in H II regions. Since there are few free electrons to collide with, and the metal atoms are more weakly ionised and thus tend to have lower energy scales, most of this line emission is in the infrared rather than the visible. The 158 μm line observed by COBE is an example of this sort of emission.

Although these IR emission lines can be used to study the WNM, as can optical and UV absorption lines, by far the most common tool is the 21 cm hyperfine transition of the hydrogen itself. This is present everywhere, and has numerous favorable features that we will discuss in a couple of weeks.

D. Cold neutral gas (CNM)

Neutral gas can be warm, but it can also be cold. The cold neutral medium, or CNM, is similar in ionisation state and energy balance to the WNM, but it is found at much lower temperatures, ~ 100 K, and much higher densities, ~ 10 cm^{-3}. Because of its high density, it has a much lower volume filling fraction, $\sim 1\%$ of the galactic disk. Nonetheless, it contains an amount of mass not much smaller than the mass of the WNM.

Why the neutral gas should have this two-temperature structure is something we will discuss in the second half of the class.

E. Diffuse molecular gas

In the densest, coldest parts of the CNM, hydrogen can become molecular. Like the transition from H I to H II this is a process driven by photons. Gas goes from neutral to ionised when there are hot stars around to provide photons above 13.6 eV. It goes from atomic to molecular regions where there is enough absorption to *exclude* photons with energies of above ~ 5 eV, the binding energy of a hydrogen molecule. Only the densest and coldest regions of CNM do this, so H_2 is found only in gas at densities ~ 100 cm^{-3} and at temperatures ~ 50 K. The volume occupied by these regions is tiny, $\sim 0.1\%$ of the disk.

Despite the transition from atomic to molecular, in the diffuse H_2 clouds the energetics are quite similar to those in CNM or WNM. Molecular hydrogen does not provide much of a source of heating or cooling, for reasons we'll discuss in a week. For the same reason, observing these regions is hard – the 21 cm H I line is unavailable, and H_2 is hard to see. The main way we know about this gas is via UV absorption lines of H_2, which are available only when there is a conveniently-located background star.

F. Dense molecular gas / GMCs

The final, densest phase is the dense molecular gas. In this part of the ISM the temperature falls to ~ 10 K or even a little lower, and the density is at least 100 cm^{-3}, and often more. Most of the gas in this state is organised in discrete structures known as giant molecular clouds. These clouds occupy only $\sim 10^{-4}$ of the volume of the galactic disc, but constitute $\sim 1/4$ of its total gas mass. In some other galaxies that fraction is even higher. These clouds are also where star formation occurs.

The change that occurs between diffuse and dense molecular gas that causes this change in properties is the appearance of molecules. Whereas in the diffuse molecular gas and all the less dense phases most of the carbon, oxygen, and other species are either atomic or in dust grains, in the dense molecular gas significant fractions of these atoms end up in diatomic and polyatomic molecules, the most prominent of which is CO.

The appearance of these molecules is significant because, unlike H_2, these molecules are strong emitters, and they are able to cool the gas in a manner much like what happens in CNM: collisions (in this case with H_2 molecules) induce transitions to an excited state, and the excited molecules then radiatively decay.

The main difference is the energy scale. Electronic transitions in atoms or molecules have energy scales of eV. For molecules, however, there are also excited states associated with rotation and vibration. Recalling our quantum mechanics, for a quantum harmonic oscillator the energy spacing between levels varies inversely with the mass of the oscillator, and the same general scaling applies to other systems. Since rotational and vibrational levels of molecules involve moving the nuclei rather than the electrons, the energy scales are generally below 10^{-3} eV, corresponding to the factor of 1000 proton-electron mass ratio. This lower energy scale means that even in $\sim$ 10 K gas there are states that can be excited by collisions.

These atomic and molecular transitions also provide the most common way of studying the dense molecular gas, particularly the rotational levels of CO. Other methods include mm emission by cold dust grains, and infrared absorption of background starlight.

IV. Collisional processes

In the final part of the class today, we will begin to build the theoretical tools we will need to understand the behavior of the ISM. The first goal will be an understanding of collisions between particles. In the materials we're used to, collisions occur so frequently that we don't usually worry about them, and we simply assume that they occur frequently enough for distributions to reach thermodynamic equilibrium. In the ISM we cannot safely make this assumption, and so we must worry about calculating the rates of collisions.

A. The collision rate coefficient

Consider an interaction between two particles A and B, which we write in the general form

$$A + B \rightarrow \text{products} \tag{1}$$

Depending on the type of interaction, the products that appear on the right hand side can be many different things. Simple elastic scattering is a trivial case, for which products is simply $A + B$ again. For inelastic scattering, where either A or B is left in an excited state after the encounter, it might be $A^* + B$ or $A + B^*$, with the asterisk indicating an excited state. If a chemical reaction occurs, it might be an entirely different species C. For now, the exact identity of the right hand side does not matter.

We wish to compute the rate at which the given reaction / collision occurs in a gas that contains species A and B with number densities n_A and n_B, respectively. The dependence of the densities is fairly obvious. Suppose we imagine a beam of particles of type A being fired at a static grid of particles of type B. Clearly the rate of collisions will be linearly proportional to both the density of targets and the density of particles in the beam. Thus we expect to have a rate per unit volume that varies as $n_A n_B$. We rate the rate as

$$\text{rate per unit volume} = n_A n_B k_{AB}, \tag{2}$$

where k_{AB} is the rate coefficient for the reaction. It has units of cm^3 s^{-1}.

By analogy one can also define three-body collision rate coefficients, for reactions involving three species such that the rate per unit volume is $n_A n_B n_C k_{ABC}$. In practice the low density of the ISM implies that three-body processes are only very rarely important.

B. Calculation of rate coefficients

To figure out k_{AB}, we can roughly divide it into two parts: the "internal" part that has to do with the physical properties of the colliding particles and the quantum mechanical probabilities of a given interaction producing a given outcome, and the "external" part that has to do with the kinematics of particles running into one another.

To see how the external part works, we can first return to the easier-to-picture case of a beam of particles directed at a static grid of targets. Clearly if the beam moves faster, more particles per unit time will go through the array of targets, so the collision rate will be linearly proportional to the relative velocity of the targets and the beam. In the more realistic case of two interacting species mixed together, we need to integrate over all possible reaction velocities. Thus we can write

$$k_{AB} = \int_0^\infty v f_v \sigma_{AB}(v)\, dv = \langle \sigma \rangle_{AB}, \tag{3}$$

where v is the relative velocity, f_v is the fraction of particle pairs that have that relative velocity, and $\sigma_{AB}(v)$ is the velocity-dependent interaction cross-section. This encapsulates all the internal information about particle sizes and quantum transition probabilities. The angle brackets indicate an average of σ over collision velocities.

We can compute f_v from the Boltzmann distribution, under the assumption (which we'll check later) that the particles follow this distribution. To remind you: the Boltzmann distribution says that in a system with temperature T, the probability of finding a particle in a state with energy E is proportional to $e^{-E/k_B T}$. Thus the probability of having a given vector velocity $\mathbf{v} = (v_x, v_y, v_z)$ is proportional to $e^{-mv^2/(2k_B T)}$, where m is the particle mass and $v = \sqrt{v_x^2 + v_y^2 + v_z^2}$, and we have

$$\frac{d^3 f}{dv_x\, dv_y\, dv_z} = \left(\frac{m}{2\pi k_B T}\right)^{3/2} e^{-mv^2/(2k_B T)}. \tag{4}$$

The normalisation constant in front has been chosen to ensure that the integral of $d^3 f/(dv_x\, dv_y\, dv_z)$ over all possible velocities is unity.

This is the velocity distribution for individual particles. In other words, it applies separately to A and B, and we have

$$\frac{d^3 f_A}{dv_{x,A}\, dv_{y,A}\, dv_{z,A}} = \left(\frac{m_A}{2\pi k_B T}\right)^{3/2} e^{-m_A v_A^2/(2k_B T)} \tag{5}$$

and similarly for B. We want to know what the probability that a randomly chosen pair of particles has relative velocity v. To compute this, first note that the probability of a given velocity combination $\mathbf{v}_A, \mathbf{v}_B$ is the just the product of the individual probabilities, the same as for any independent pair of events. Thus

$$\frac{d^6 f(\mathbf{v}_A, \mathbf{v}_B)}{d\mathbf{v}_A\, d\mathbf{v}_B} \propto \left(\frac{\sqrt{m_A m_B}}{2\pi k_B T}\right)^3 e^{-(m_A v_A^2 + m_B v_B^2)/(2k_B T)}. \tag{6}$$

This is a six-dimensional probability distribution function that gives us the probability of picking a given sextuplet of values $(\mathbf{v}_A, \mathbf{v}_B)$. What we want to know is the probability of picking a sextuplet that has the particular property that $|\mathbf{v}_A - \mathbf{v}_B| = v$, since that is the definition of f_v. Thus we want to compute

$$\int e^{-(m_A v_A^2 + m_B v_B^2)/(2k_B T)} \delta(|\mathbf{v}_A - \mathbf{v}_B| - v)\, d^3\mathbf{v}_A\, d^3\mathbf{v}_B. \tag{7}$$

We've dropped the leading constants because we're only interested in the dependence on velocities – other coefficients we can recompute at the end just by requiring that our integrated probability be unity.

This integral can be evaluated by making a change of variables. Let $\mathbf{v} = \mathbf{v}_A - \mathbf{v}_B$, and $\mathbf{v}_{\mathrm{CM}} = (m_A \mathbf{v}_A + m_B \mathbf{v}_B)/(m_A + m_B)$, or equivalently

$$\mathbf{v}_A = \frac{\mu}{m_A}\mathbf{v} + \mathbf{v}_{\mathrm{CM}} \qquad \mathbf{v}_B = -\frac{\mu}{m_B}\mathbf{v} + \mathbf{v}_{\mathrm{CM}} \qquad \mu = \frac{m_A m_B}{m_A + m_B} \tag{8}$$

First hold $\mathbf{v}$ and $\mathbf{v}_A$ fixed and substitute for $\mathbf{v}_B$ in terms of $\mathbf{v}_{\mathrm{CM}}$; in this case $d^3\mathbf{v}_B = -(\mu/m_B)^3 d^3\mathbf{v}_{\mathrm{CM}}$, and the integral becomes

$$\int \exp\left[-\frac{m_A v_A^2 + m_B |(\mu/m_B)\mathbf{v} - \mathbf{v}_{\mathrm{CM}}|^2}{2k_B T}\right] \delta\left(\left|\mathbf{v}_A + \frac{\mu}{m_B}\mathbf{v} - \mathbf{v}_{\mathrm{CM}}\right| - v\right) d^3\mathbf{v}_A\, d^3\mathbf{v}_{\mathrm{CM}}, \tag{9}$$

where we have again dropped leading constants that don't depend on velocity. Now hold $\mathbf{v}_{\mathrm{CM}}$ fixed and substitute for $\mathbf{v}_A$ using $\mathbf{v}$. Thus $d^3\mathbf{v}_A = (\mu/m_A)^3 d^3\mathbf{v}$, and the integral becomes

$$\int \exp\left[-\frac{m_A |(\mu/m_A)\mathbf{v} + \mathbf{v}_{\mathrm{CM}}|^2 + m_B |(\mu/m_B)\mathbf{v} - \mathbf{v}_{\mathrm{CM}}|^2}{2k_B T}\right] \delta\left(|\mathbf{v}| - v\right)\, d^3\mathbf{v}\, d^3\mathbf{v}_{\mathrm{CM}}. \tag{10}$$

Now it's just a matter of algebra to evaluate the integral. The term in the exponential can be expanded to

$$m_A \left| \frac{\mu}{m_A} \mathbf{v} + \mathbf{v}_{\mathrm{CM}} \right|^2 + m_B \left| \frac{\mu}{m_B} \mathbf{v} - \mathbf{v}_{\mathrm{CM}} \right|^2 = \frac{\mu^2 v^2}{m_A} + \frac{\mu^2 v^2}{m_B} + (m_A + m_B) v_{\mathrm{CM}}^2 \tag{11}$$

$$= \mu v^2 + (m_A + m_B) v_{\mathrm{CM}}^2, \tag{12}$$

and if we substitute this in we get

$$\int \exp\left[-\frac{\mu v^2}{2k_B T}\right] \exp\left[-\frac{(m_A + m_B) v_{\mathrm{CM}}^2}{2k_B T}\right] \delta\left(|\mathbf{v}| - v\right) \, d^3\mathbf{v} \, d^3\mathbf{v}_{\mathrm{CM}} \tag{13}$$

The part that depends on v and not v_{CM} is now trivial to evaluate thanks to the δ function, which just gives us a v^2 dependence:

$$v^2 \exp\left(-\frac{\mu v^2}{2k_B T}\right) \int \exp\left[-\frac{(m_A + m_B) v_{\mathrm{CM}}^2}{2k_B T}\right] d^3\mathbf{v}_{\mathrm{CM}} \tag{14}$$

The remaining integral is just a number that does not depend on velocity, and so we've arrived at the fundamental dependence we were after: $f_v \propto v^2 e^{-\mu v^2/2k_B T}$. Inserting the appropriate normalization factor to ensure that the integral over all velocities gives unity, we have

$$f_v = 4\pi \left(\frac{\mu}{2\pi k_B T}\right)^{3/2} v^2 e^{-\mu v^2/2k_B T}. \tag{15}$$

The two-body collision rate coefficient therefore is

$$k_{AB} = 4\pi \left(\frac{\mu}{2\pi k_B T}\right)^{3/2} \int_0^\infty v^3 e^{-\mu v^2/2k_B T} \sigma_{AB}(v) \, dv. \tag{16}$$

Alternately, it is sometimes helpful to write things in terms of the energy of the collision in the center of mass frame instead of the relative velocity. The distribution in energy is just given by the fundamental rule for the transformation of probabilities: $f_v \, dv = f_E \, dE$, i.e. since E is a monotonic function of v, the probability of measuring a velocity between v and $v + dv$ must be the same as the probability of measuring an energy between E and $E + dE$. Since $E = \mu v^2/2$ and $v = \sqrt{2E/\mu}$, we have $dE = \mu v \, dv$, and plugging in we get

$$k_{AB} = \sqrt{\frac{8k_B T}{\pi\mu}} \int_0^\infty x e^{-x} \sigma_{AB}(x k_B T) \, dx, \tag{17}$$

where $x = E/k_B T$. This is often the most practical form for computation.

The function we have just written down already carries an important point. Suppose we have a cross section that is not highly velocity- or energy-dependent. In this case σ_{AB} is a constant and comes out of the integral. The remaining part, the integral of xe^{-x} from 0 to ∞, trivially evaluates to 1, and we have

$$k_{AB} = \sqrt{\frac{8k_B T}{\pi\mu}}\sigma_{AB}. \tag{18}$$

This gives us a simple formula to evaluate any reaction coefficient with a constant cross section, and shows us that such reactions proceed at a rate that varies as $T^{1/2}$. In practice it turns out that there are reasonably large number of collisional processes where the cross section is indeed not very energy-dependent, so in practice many rate coefficients do vary as close to $T^{1/2}$.

C. Cross sections and rate coefficients for varying reactant types

Now that we have a general framework, we are in a position to work out reaction rate coefficients for a variety of interaction types.

1. Neutral-neutral scattering

The simplest case to consider is scattering of one neutral species off another. For now we will not worry if the interaction is elastic or not, and we will simply compute the overall collision rate; the elastic and inelastic interaction rates will each be a fraction of this total rate. This collision rate is particularly important because interactions of this sort are responsible for establishing a Boltzmann distribution of velocities among a population of neutral particles, which is what we assumed existed for the purposes of computing rate coefficients.

At large distances the only force between two neutral particles is a van der Waals attraction, produced when fluctuations in the electric dipole moment of one particle induce a corresponding electric dipole in the other. Since the dipole electric field of the first particle varies as $1/r^3$, so does the strength of the dipole in the second particle. The potential then varies as the product of the two dipoles, giving rise to an overall potential that varies as $1/r^6$. Moreover, since the dipole is only due to fluctuations, the coefficient is quite small. When the two particles get within ~ 1 Å of one another, i.e. when the separation is comparable to the total sizes of the interacting molecules or atoms, the electron clouds of the two neutrals begin to repel one another, and the force becomes very strongly repulsive.

This combination of very weak attraction at large radii, coupled with a sudden transition to strong repulsion at small separations, can be modeled reasonably well as a "hard sphere" interaction. We simply think of the two neutrals as balls with a physical size of $r_A = r_B = 1$ Å; if they get closer than 2 Å they collide, and otherwise they do not. Thus

$$\sigma_{AB} = \pi(r_A + r_B)^2 = 1.2 \times 10^{-15} \text{ cm}^2. \tag{19}$$

Plugging this into our trivial expression for the rate coefficient when the cross section is constant, we get

$$k_{AB} = 1.81 \times 10^{-10} \left(\frac{T}{100\,\mathrm{K}}\right)^{1/2} \left(\frac{m_\mathrm{H}}{\mu}\right)^{1/2} \left(\frac{r_A + r_B}{2\ \text{Å}}\right)^2 \ \mathrm{cm}^3\ \mathrm{s}^{-1}. \tag{20}$$

We can think of this as a generic, order-of-magnitude estimate for the collision rate coefficient for any process where the particles are neutral and there are no chemical reactions involved, just scattering.

2. Charged-neutral scattering

Now let us consider the interaction of a neutral particle with a charged one. This could be a neutral atom or molecule interacting either with an ion or with a free electron. The main difference here is that the force when the two particles are far apart is no longer completely negligible. Let us suppose that the charged particle has a charge Ze, where e is the electron charge. The electric field of the charged particle will polarize the neutral particle, inducing a dipole moment $\mathbf{P} = \alpha \mathbf{E}_\mathrm{ch}$, where α is the polarizability of the neutral particle and $\mathbf{E}_\mathrm{ch}$ is the electric field created by the charged particle. Typical polarizabilities are of order a_0^3, where $a_0 = \hbar^2/m_e e^2 = 5.29 \times 10^{-9}$ cm is the Bohr radius. These can be computed quantum mechanically or measured in the lab fairly easily.

The attractive force that the polarized atom experiences is given by the standard formula for the force on a dipole in an electric field: $F = P(dE_\mathrm{ch}/dr) = -2\alpha Z^2 e^2/r^5$. The corresponding interaction potential is

$$U(r) = -\frac{1}{2}\frac{\alpha Z^2 e^2}{r^4}. \tag{21}$$

Scattering in an r^{-4} potential has the property that there is a critical impact parameter b_0 (defined as the distance of closest approach that the two particles would have if there were no force between them) below which the separation between the two particles goes through zero exactly. (Proving this is left as an exercise to the reader – it's fairly easy to show simply by writing down the Largangian for the system.) Deflections are relatively weak for larger impact parameters.

The value of b_0 depends on the relative energy of the two particles at infinity in the center of mass frame, E. It is given by

$$b_0 = \left(\frac{2\alpha Z^2 e^2}{E}\right)^{1/4} = 6.62 \times 10^{-8} Z^{1/2} \left(\frac{\alpha}{\alpha_\mathrm{H}}\right)^{1/4} \left(\frac{0.01\ \mathrm{eV}}{E}\right)^{1/4}\ \mathrm{cm}, \tag{22}$$

where $\alpha_\mathrm{H} = 4.5 a_0^3$ is the polarizability of neutral hydrogen. Thus we see that in general b_0 is significantly larger than the $\sim 10^{-8}$ cm geometric cross section of the particles. This means that πb_0^2 provides a natural estimate for the collision cross section of an ion and a neutral, since any interaction in which the initial impact parameter is below b_0 will necessarily bring the ion and neutral extremely close, while more distant interactions will not produce significant interaction. Plugging this in, we have

$$\sigma_{AB} = \pi b_0^2 = \pi Ze\sqrt{\frac{2\alpha}{E}} \tag{23}$$

Plugging this into our expression for the rate coefficient, we have

$$\begin{aligned}
k_{AB} &= \sqrt{\frac{8k_BT}{\pi\mu}} \int_0^\infty xe^{-x} \left(\pi Ze\sqrt{\frac{2\alpha}{xk_BT}}\right) dx && (24)\\
&= 4Ze\sqrt{\frac{\pi\alpha}{\mu}} \int_0^\infty x^{1/2}e^{-x}\, dx && (25)\\
&= 2\pi Ze\sqrt{\frac{\alpha}{\mu}} && (26)\\
&= 8.98\times 10^{-10} Z \left(\frac{\alpha}{a_0^3}\right)^{1/2} \left(\frac{m_\mathrm{H}}{\mu}\right)^{1/2} \mathrm{cm}^3\ \mathrm{s}^{-1}. && (27)
\end{aligned}$$

Note that the result is independent of temperature. This means that, even at low temperatures where neutral-neutral collisions are very rare (due to the $T^{1/2}$ dependence), ion-neutral collisions continue to remain common. This makes ion-neutral reactions a critical driver of chemistry in low-temperature gas.

3. Charged-charged collisions

   Collisions between two charged particles are a bit more complicated, because there we have a long-range force, and even at large distances there will be some non-negligible transfer of momentum. A useful approximation in this case is the impact approximation. The basic idea of the impact approximation is simple: we neglect changes in particle velocities during the encounter, and simply add up the change in transverse momentum that a projectile particle experiences as a result of the forces exerted by the electric field of the target. (The net change in momentum along the direction of the encounter is zero.)

   The setup is simple: consider two particles of charges Z_1e and Z_2e, and work in the reference frame where particle 2 is at rest. Particle 1 approaches it, moving with velocity v_1 and with impact parameter b. Following the impact approximation, it moves in a straight line at constant velocity v_1 independent of how close it gets to particle 2. Let x be the distance between particle 1 and the point of closest approach, and θ be the angle between the line of closest approach at the line between the two particles at any given time.

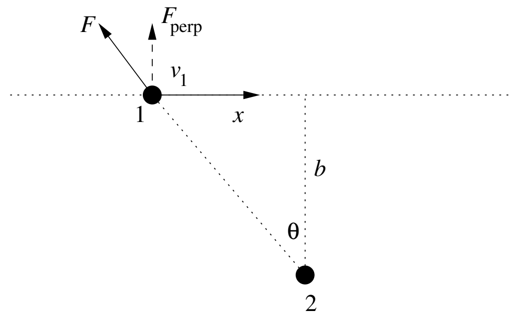

At a time when the angle between the two particles is θ, the distance between them is $b/\cos\theta$, so the total force is $F = Z_1 Z_2 e^2/(b/\cos\theta)^2$. The component of this in the perpendicular direction is $\cos\theta$ of the total, so the total perpendicular force is

$$F_\perp = \frac{Z_1 Z_2 e^2}{b^2}\cos^3\theta. \tag{28}$$

To figure out the total momentum imparted over the entire encounter, we must find out how much time the particle spends at each angle θ, since $dp/dt = F$. This is easy to compute: clearly $x = b\tan\theta$, and

$$v_1 = \frac{dx}{dt} = b\frac{d}{dt}\tan\theta = \frac{b}{\cos^2\theta}\frac{d\theta}{dt} \qquad \Rightarrow \qquad d\theta = \frac{v_1}{b}\cos^2\theta\, dt. \tag{29}$$

Now it's just a matter of integrating over time to get the total momentum change:

$$\Delta p_\perp = \int_{-\infty}^{\infty} F_\perp\, dt = \frac{Z_1 Z_2 e^2}{b^2}\int_{-\infty}^{\infty}\cos^3\theta\, dt = \frac{Z_1 Z_2 e^2}{b v_1}\int_{-\pi/2}^{\pi/2}\cos\theta d\theta = 2\frac{Z_1 Z_2 e^2}{b v_1}. \tag{30}$$

So what does this tell us about the cross section? It tells us that we need to think carefully about what exactly we mean. Notice that the transverse momentum change varies as $1/b$, so more distant encounters have more effect. That's good. However, the total area available for encounters goes as $2\pi b\, db$, i.e. there's also more area available at large b than small b. The product of area times effect, $2\pi b\, db \cdot \Delta p_\perp$, does not depend on b, and if we integrate over all impact parameters from zero to infinity, things diverge! This means that the encounter cross section as we've been thinking about it in the neutral-neutral and neutral-charged cases is not really a meaningful concept as applied to the charged-charged case. We need to be a bit more specific about what sort of encounter we're interested in.

4. Electron-ion collisions and collision strengths

One problem of great interest is figuring out when a collision between an ion or atom and an electron will induce a change in the quantum state of the ion, either an excitation or de-excitation. (We will see in the next class that if you know the rate of one, you automatically know the other as well.) Such collisionally-induced changes in state, followed by radiative decay of excited states, are responsible for most of the visually-spectacular emission we need from ionised nebulae. We specialise to the case of an electron because electrons generally move much faster than ions, so most collisions are electron-ion rather than ion-ion.

Consider an encounter between an ion of charge Z and an electron. The unperturbed ion has a potential $U(r)$ in which the electrons move. We'll do the case of collisional de-exciation, so let the ion be in some excited eigenstate u of the potential $U(r)$, with energy E_u. We want to know the rate at which collisions cause it to transition to a lower energy state ℓ with energy E_ℓ.

We can calculate this rate up to a factor of order unity using a semi-classical approach. Here we will not use the impact approximation, and we will include deflection of the electron by the ion potential. Suppose the approaching electron moves classically in the potential provided by the ion. What is its closest approach? If the electron approaches with initial velocity v and impact parameter b, then its initial energy is $m_e v^2/2$ and its initial angular momentum is $m_e v b$. Conservation of energy and angular momentum then imply that at the point of closest approach $r_{\min}$ and maximum velocity $v_{\max}$, we have

$$\begin{aligned} \frac{1}{2} m_e v^2 &= \frac{1}{2} m_e v_{\max}^2 - \frac{Z e^2}{r_{\min}} && (31) \\ m_e v_{\max} r_{\min} &= m_e v b. && (32) \end{aligned}$$

From these two conditions and a little algebra, it is easy to show that

$$b = r_{\min} \left(1 + \frac{2 Z e^2}{m_e v^2 r_{\min}}\right)^{1/2}. \tag{33}$$

How close does the electron have to get to have a significant chance of inducing a state change? At the order of magnitude level, the answer is that the perturbation in the potential δU must be comparable to or larger than the difference in energy between the two levels $E_{u\ell} = E_u - E_\ell$. Thus we want the distance of closest approach to obey

$$\frac{e^2}{r_{\min}} \sim E_{u\ell}. \tag{34}$$

It is convenient to normalise the energy difference to typical energy differences for electronic states. The typical energy scale for two electronic states is of order the potential of an electron at a distance of order a Bohr radius, i.e. $E_{u\ell} \sim e^2/a_0$ for a typical pair of electronic states. We therefore adopt a minimum distance

$$r_{\min} = W a_0, \tag{35}$$

where W is a constant whose value will depend on the exact transition. For electronic transitions that produce optical lines, we expect it to be of order unity.

Plugging this in for $r_{\rm min}$, we obtain a maximum impact parameter required to have a reasonable chance of inducing a change in state:

$$b_{\rm max} \approx W a_0 \left(1 + \frac{2Ze^2}{m_e v^2 W a_0}\right)^{1/2}. \tag{36}$$

The corresponding cross section is

$$\sigma_{u\ell} = \pi b_{\rm max}^2 = W^2 \pi^2 a_0^2 \left(1 + \frac{2Ze^2}{m_e v^2 W_0 a_0}\right). \tag{37}$$

Now we just have to integrate over the Maxwellian velocity distribution to get the rate coefficient:

$$\begin{aligned} k_{u\ell} &= 4\pi \left(\frac{\mu}{2\pi k_B T}\right)^{3/2} \int_0^\infty v^3 e^{-\mu v^2/2k_B T} W^2 \pi^2 a_0^2 \left(1 + \frac{2Ze^2}{m_e v^2 W_0 a_0}\right) dv \qquad (38) \\ &= \pi W^2 a_0^2 \left(\frac{8 k_B T}{\pi m_e}\right)^{1/2} \left(1 + \frac{Ze^2}{W a_0 k_B T}\right), \qquad (39) \end{aligned}$$

were we have again set $\mu = m_e$.

The term $Ze^2/(a_0 k_B T)$ that appears in the second parentheses has the numerical value $15.78(Z/T_4)$, where T_4 is the temperature in units of 10^4 K. Thus unless $Z/T_4 \ll 1$, which is generally not the case in optical nebulae, we can drop the 1. Doing so and recalling that $a_0 = \hbar^2/(m_e e^2)$, we obtain

$$k_{u\ell} \approx \frac{h^2}{(2\pi m_e)^{3/2}} \frac{1}{(k_B T)^{1/2}} 2WZ. \tag{40}$$

Thus we have written the collision rate in terms of the unknown parameter W, which is a measure of how easy it is to perturb the atom. Based on this argument, we formally define the dimensionless **collision strength** $\Omega_{u\ell}$ of a particular interaction by

$$k_{u\ell} \equiv \frac{h^2}{(2\pi m_e)^{3/2}} \frac{1}{(k_B T)^{1/2}} \frac{\Omega_{u\ell}}{g_u}. \tag{41}$$

The reason for including the factor of g_u, the degeneracy of the upper state, will become apparent when we discuss the statistical mechanics of collisions. The advantage of this definition of $\Omega_{u\ell}$ is that it "factors out" the dependence of the reaction rate on the kinetics of the plasma, which is essentially the same for any reaction, and isolates the quantum-mechanical part that is reaction-specific.

Collision strengths must be calculated quantum mechanically or measured in the laboratory. Exact values are generally known only to the $\sim 10\%$ level, except for a few very well-studied cases. Unfortunately many of the astrophysically relevant collisions are quite difficult to study on Earth, because the lines they correspond to are very weak and hard to see under terrestrial conditions. Also note that in general $\Omega_{u\ell}$ can be a function of temperature, but in practice it is at most a very weak one, and the temperature dependence can be dropped.